Development and Assessment of CTF for Pin-Resolved BWR Modeling

R. Salko[1], A. Wysocki[1], B. Collins[1], M. Avramova[2], and C. Gosdin[3]

[1]Oak Ridge National Laboratory
[2]North Carolina State University
[3]The Pennsylvania State University

Abstract — *CTF is the modernized and improved version of the subchannel code COBRA-TF. It has been adopted by the Consortium for Advanced Simulation for Light Water Reactors (CASL) for subchannel analysis applications and thermal hydraulic feedback calculations in the Virtual Environment for Reactor Applications Core Simulator (VERA-CS). CTF is now jointly developed by Oak Ridge National Laboratory and North Carolina State University. Until now, CASL has used CTF for pressurized water reactor modeling and simulation, but in the future CTF will be extended to boiling water reactor designs. This required development activities to integrate the code into the VERA-CS workflow and to make it more efficient for full-core, pin-resolved simulations. Additionally, in conformance with the CASL software quality assurance plan, CTF had to be assessed for its intended application by performing validation and verification testing. Furthermore, these tests must be easily repeatable and tied to a specific version of the code. This work has resulted in the CTF validation and verification matrix being expanded to include several two-phase flow experiments, including the General Electric 3 × 3 facility and the BWR Full-Size Fine Mesh Bundle Tests. Comparisons with both experimental databases is reasonable, but the bundle test analysis reveals CTF's tendency to overpredict void, especially in the slug flow regime. The execution of these tests is fully automated, analysis is documented in the CTF validation and verification manual, and the tests have become part of CASL continuous regression testing system. This paper summarizes these recent developments and some of the two-phase assessments that have been performed on CTF.*

I. INTRODUCTION

CTF [1] is a modernized and improved version of the legacy subchannel code, COBRA-TF [2], which is being jointly developed and maintained by Oak Ridge National Laboratory (ORNL) and North Carolina State University. The code was adopted by ORNL for use in the Consortium for Advanced Simulation of Light Water Reactors (CASL) in 2012 for aiding in addressing CASL challenge problems. Since that time, activities related to CTF have included implementing software quality assurance measures, implementing new features and models, performing validation and verification testing, establishing and supporting a CTF user group, and developing the code for use in coupled applications [3, 4, 5]. The code has also been coupled to the neutron transport code, MPACT [6], in the core simulator, Virtual Environment for Reactor Applications Core Simulator (VERA-CS), being developed by CASL [7] for providing thermal feedback in reactor cycle depletions. Other multiphysics applications of CTF includes coupling to the crud-chemistry code, MAMBA and MPACT in VERA-CS for modeling of crud-induced power shift (CIPS) [8] as well as coupling to the fuel-performance code, Bison and MPACT in the multiphysics package, Tiamat being developed by CASL [9].

The continuous development and support of the code

has led to growth in the CTF user base and applications in academia and industry. CTF is applicable to single- and two-phase flows in light water reactor geometries at normal and accident operating conditions. A transient two-fluid model is used to model two-phase flow with the liquid phase being divided into a continuous liquid and droplet field, which allows the independent behavior of fluid film and droplets to be captured. The solution methodology of the code was originally developed with the intent it would be primarily applied to modeling reactor accident conditions, which must account for high void flows and post critical heat flux. Development of CTF in CASL is focused on improving the code for normal reactor operating conditions in both pressurized water reactors (PWRs) and boiling water reactors (BWRs), as well as for departure for nucleate boiling margin analysis and CIPS.

This paper discusses recent developments and assessment of CTF for the modeling of BWR conditions in VERA-CS. First, a new preprocessor utility that is capable of handling BWR-specific design elements (e.g., channel boxes and large water rods) is developed. The purpose of this preprocessor is to generate native CTF input decks from a reduced amount of core design information as specified in the intuitive, user-friendly VERAIn input format [10]. The preprocessor creates multiassembly BWR models at a pin-cell resolution.

Second, CTF was modified by implementing an outer-iteration loop, specific to BWR models, that acts to equalize the pressure loss over all assemblies in the core by adjusting inlet mass flow rate. This loop was not needed for PWR models because the assemblies were connected, which allows for

pressure to naturally equalize. To demonstrate the successful functioning of these two improvements a demonstration of using CTF for a full-core, pin-resolved, steady-state simulation of a BWR core is presented.

Third, the CTF validation and verification (V&V) manual [11] has been expanded to include modeling of several experimental facilities that include two-phase flow. These include the General Electric (GE) 3 × 3 facility [12] and the BWR Full-Size Fine-Mesh Bundle Tests (BFBT) facility [13]. While CTF has been used to model these facilities in the past [14, 15], the results of these previous assessments have not been linked to a specific code version that is maintained in a change-control system. This current assessment was important because 1) it was done using the latest version of CTF, which is used in VERA-CS by CASL and maintained in the Git version control system (significant changes have been made to the underlying code structure and new models, like the Thom boiling model, have been added); 2) the assessment process was completely automated using Python scripts, from building CTF models, to running them, extracting results, and generating plots and statistics; 3) many of the V&V cases are included in the CASL continuous testing system, meaning they are run on a daily basis on the CASL testing machine that ensures results do not change; and 4) all results are collected in the CTF V&V manual, giving the end user confidence in the capabilities and limitations of the specific code version they are using. Furthermore, through this work, areas for code modeling improvements have been discovered and are being used to drive future CASL development activities.

This paper summarizes work that has been done to integrate CTF into the VERA-CS workflow for modeling BWRs and CTF changes that were made to allow for modeling large-scale, pin-resolved BWR models. An overview of the assessment of CTF void content and distribution predictive capabilities is also given by comparing to the GE and BFBT facility results.

II. BWR PREPROCESSOR

CTF models used in VERA-CS simulations are created at the pin-resolution level. As a result, these models often contain tens of thousands of channels and rods and, thus, millions of mesh cells for core-scale models. All of these model entities must be explicitly defined in the native CTF input deck, leading to very large input decks. Because manually creating such large models would be impractical, CASL has developed a separate preprocessor utility that generates native CTF input decks from the reduced, user-friendly input of the VERAIn common input file. Originally, this preprocessor was developed for creating PWR models only. This work extends the preprocessor to include BWR-specific designs.

The preprocessor supports multiple pin and fuel types and multiple assembly types that may have different lattice sizes and different spacer grid placement. It also supports large water rods that take up multiple pin cells in the model. The utility will also generate a postscript file that shows a top-view picture of the model generated, including pin and channel indices as specified in the CTF model. This feature helps the user see what they will actually be modeling when they run
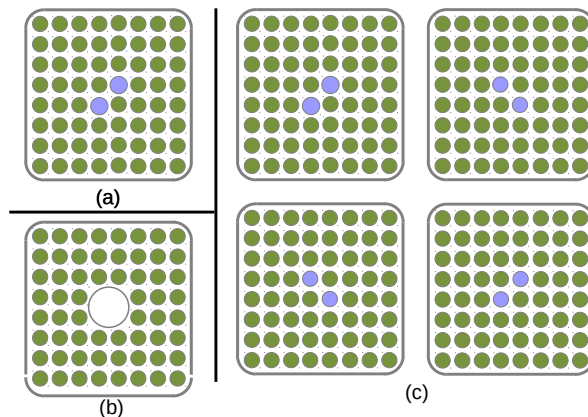

Fig. 1. Geometry of preprocessor regression tests.

the simulation in CTF. In the future, a feature will be added to treat the presence of partial-length rods in the model. The bypass will be treated by specifying a constant percentage of flow in the bypass region via user input. Sensitivity studies will be performed to determine if it is necessary to explicitly model this region and heat transfer between the in-bundle and bypass regions of the core.

The preprocessor is tested by designing a collection of BWR single- and multiple-assembly regression tests. The preprocessor is used to generate CTF models from the VERAIn file, and then the resulting CTF input file is hand-checked and verified to be correct. The verified CTF input decks are used as "gold files." Automated regression tests are setup using CMake and TriBITS to automatically run the preprocessor on the regression tests and check that resulting CTF input files are identical to the gold files. These tests are run on a continual basis on CASL development clusters as well as every time new code changes are checked into the master version of the repository. The geometry of the three types of current regression tests are shown in Fig. 1. Figure 1 includes the following regression tests: (a) a single 8 × 8 BWR assembly with two single-pin-cell water rods, (b) a single 8 × 8 BWR assembly with a larger water rod in the center that spans four pin-cell locations, and (c) a model of four 8 × 8 BWR assemblies that are correctly rotated as they would be in a real BWR core.

III. CTF OUTER ITERATION LOOP

The assemblies in the multiassembly models are completely separate from one another as a result of the channel boxes present around the assemblies. The models do not connect at the inlet or outlet because a lower or upper plenum is not included in the CTF model. It is possible to connect the assemblies using a lower and upper plenum, but the resulting pressure matrix will have equations with thousands of elements, which may lead to very long solution times.

A more straightforward solution is to implement an outer iteration loop in the code. The following method is used for BWR models. Once the solution reaches steady state, the code checks if the pressure drop in all assemblies matches a specified tolerance range. If not, the code adjusts the assembly inlet mass flow rates and does another iteration in the outer
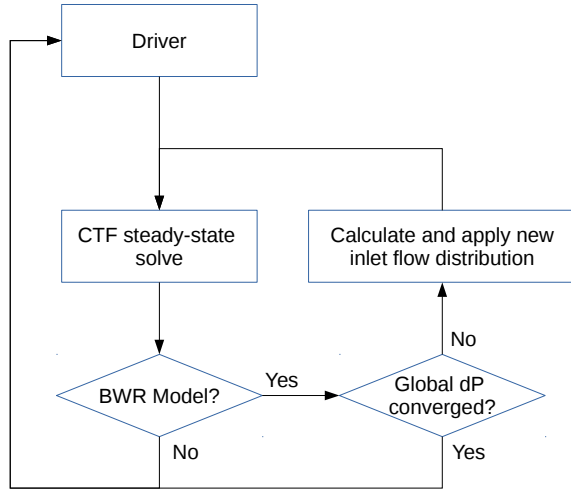
Fig. 2. Flowchart of the outer iteration loop that has been implemented in CTF for BWR models.

loop. The pressure drop stopping criteria is set to a relatively small pressure of 0.7 kPa (0.1 psi). This process is summarized in the flow chart in Fig. 2.

The inlet mass flow rate adjustments are done using a simple linear relationship between inlet mass flow rate and bundle pressure drop shown in Eq. 1:

$$\Delta P_b = C_{0,b} + C_{1,b}\dot{m}_b. \tag{1}$$

The coefficients of the correlation are C_0 (kPa) and C_1 (kPa s kg^{-1}), which are calculated during the simulation using the inlet mass flow rate and the resulting assembly pressure drop. The b subscript stands for "bundle" and indicates that one correlation is built for each fuel assembly in the model. The pressure drop over the bundle is ΔP_b, and $\dot{m}$ is the inlet mass flow rate of the bundle. At the end of the first iteration, there will not be enough data to calculate the coefficients in Eq. 1, so the inlet mass flow rate is adjusted by 5 % and another iteration is done. At the end of the second iteration, the known inlet mass flow rate, $\dot{m}_b$, and resulting pressure drop, ΔP_b, are used to determine the values of C_0 and C_1.

To use Eq. 1 to calculate the new inlet mass flow rate, it is first rearranged as shown in Eq. (2):

$$\dot{m}_b = \frac{\Delta P_b - C_{0,b}}{C_{1,b}}. \tag{2}$$

The sum of the individual assembly inlet mass flow rates should provide the total specified core inlet mass flow rate. Additionally, the pressure drop over the core should be equal in all assemblies. As Eq. (3) shows, these two facts allow the sum of the individual bundle equations to be used to predict the final core pressure drop.

$$\Sigma_{b=1}^B \dot{m}_b = \dot{m}_{core} = \Sigma_{b=1}^B \frac{\Delta P_{core} - C_{0,b}}{C_{1,b}}, \tag{3}$$
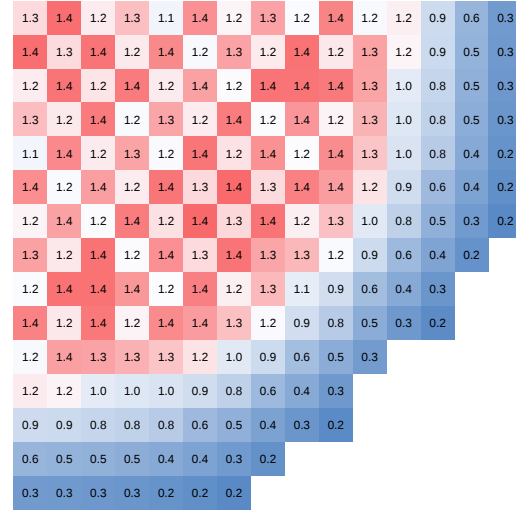

Fig. 3. Assembly peaking factors for mock BWR/4 model. Only one quarter of the model is shown.

where B is the total number of assemblies in the core, $\dot{m}_{core}$ is the total active flow into the model, and ΔP_{core} is the predicted final pressure drop over the core. Solving for the core pressure drop yields Eq. (4):

$$\Delta P_{core} = \frac{\dot{m}_{core} + \Sigma_{b=1}^B \frac{C_{0,b}}{C_{1,b}}}{\Sigma_{b=1}^B \frac{1}{C_{1,b}}}. \tag{4}$$

After the final total core pressure drop is calculated, this term is simply substituted back into Eq. 2, as ΔP_{core} should be equal to ΔP_b in the converged solution, to get the predicted required bundle inlet mass flow rate to produce this pressure drop.

IV. FULL-CORE BWR MODEL

A full-core model with 764 assemblies was created to test the outer iteration algorithm and the BWR preprocessor. The model contains roughly 61,000 subchannels, 3 million fluid mesh cells, and 48 million solid mesh cells. The radial power distribution was made nonuniform on the assembly level, and the radial power distribution within an assembly was uniform (with the exception of the guide tubes, which had zero power). Figure 3 shows the assembly peaking factors for the model. The figure only shows the peaking factors for a quarter of the model, but the full core was modeled. The axial power distribution was a modified cosine shape that was adjusted to be more bottom peaked to represent the effect of large amounts of void in the upper portion of the core. Figure 4 shows the axial power shape that was applied to all rods in the model. Information used to construct the model is shown in Table I. The assembly shown in Fig. 1(a) was used for all assemblies in the mock BWR/4 model.
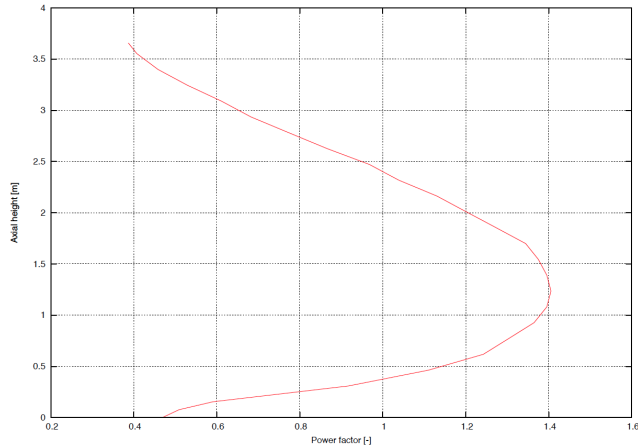
Fig. 4. Axial peaking factor shape for all rods in mock BWR/4 model.

Fig. 5. Isometric view of core equilibrium quality distribution.

TABLE I. Mock BWR/4 model data

Parameter	Value
Inlet active flow	$12\,200\,\mathrm{kg\,s^{-1}}$
Rated power	3514 MW
Gamma heating	2 %
Outlet pressure	71.70 bar
Inlet temperature	276.9 °C
Number of assemblies	764
Assembly pitch	15.24 cm
Core active length	365.76 cm
Assembly size	8×8
Pin pitch	1.6256 cm
Channel box radius	0.254 cm
Number of guide tubes per assembly	2
Fuel rod radius	0.613 41 cm
Guide tube radius	0.750 57 cm
Number of spacer grids	7
Grid loss coefficient	0.9070
Number of axial levels	49
Number of subchannels	61,884
Fluid mesh cells	3,032,316
Solid mesh cells	48,938,784

The simulation was performed on the Oak Ridge Leadership Computational Facility (OLCF) Titan cluster and used 764 processors (one for each assembly in the model). The model took five iterations of the pressure loop to converge on a single core pressure drop. The stopping criteria for each inner iteration loop was for the void, pressure, fluid temperature, solid temperature, and liquid velocity l_∞-norms less than $1.0 \cdot 10^{-4}$ and the vapor and droplet velocities to be less than $1.0 \cdot 10^{-3}$. The vapor and droplet stopping criteria were relaxed to speed up simulation time. The simulations took roughly 45 min wall-clock time to complete, which is substantially longer than a comparable PWR case. This is because the two-phase flow requires additional iterations to reach convergence
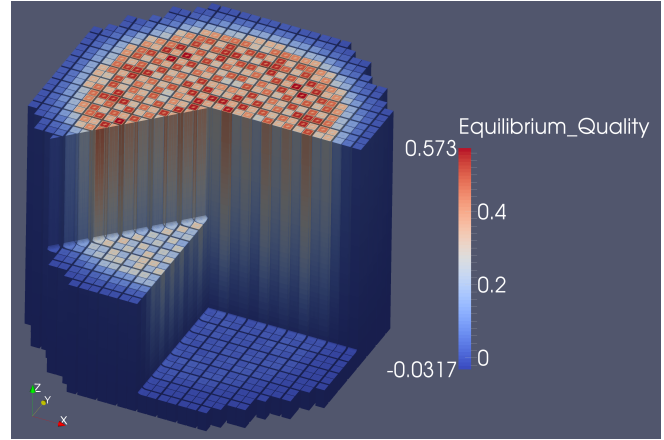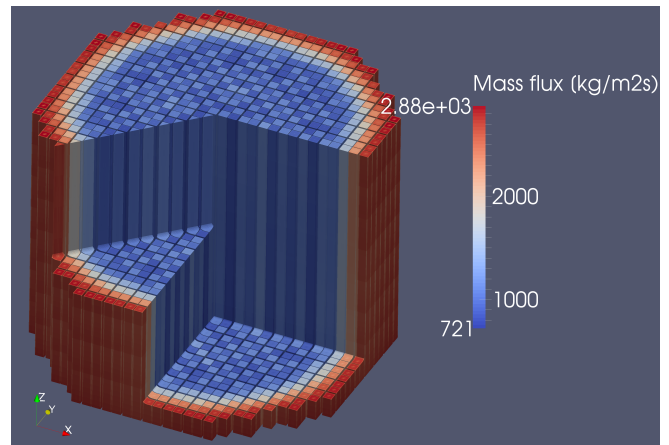

Fig. 6. Isometric view of core mixture mass flux distribution.

and also because it actually involves five CTF solves instead of just one.

Figure 5 shows an isometric view of the core with equilibrium quality distribution shown. The figure shows very low quality in outer assemblies and much higher quality in the interior of the core. This effect is a result of a large two-phase pressure drop in the high-power interior assemblies causing flow to migrate to the outside of the core. No inlet orificing was applied to this model to reduce this effect, so mass flux in the periphery assemblies is about a factor of three larger than the interior assemblies. Figure 6 presents an isometric view of the mixture mass flux distribution through the core.

These results demonstrate that CTF can now be used for pin-resolved simulation of full-core BWR models. Future work will involve optimizing the pressure loop algorithm. Performance can likely be significantly improved by using a simple drift-flux solver to precalculate the core inlet mass flow rate distribution and, thus, reduce the required number of iterations in the pressure loop.
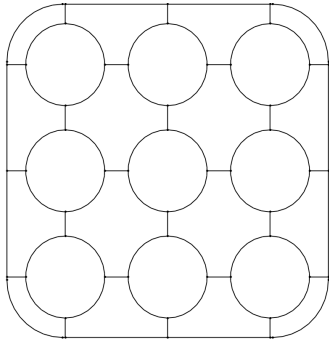
Fig. 7. GE 3×3 cross section and CTF channel layout.

V. TWO PHASE FLOW ASSESSMENT

1. GE 3×3

The GE 3×3 facility is an electrically heated 9-rod facility that uses steam as the working fluid. Bundle geometry was representative of BWR designs, including the corner round found in fuel channel box. The operating conditions were also consistent with prototypical BWR operating conditions. The cross-section of the facility and the CTF subchannel layout is shown in Fig. 7.

These experiments test CTF's ability to predict the mass and energy redistribution in rod bundle geometry. The models that have the most impact on outlet mass flux and enthalpy distribution are the wall friction model, turbulent mixing model, interfacial drag model, and void drift model. The CTF turbulent mixing model is a simple turbulent diffusion approximation with a two-phase multiplier for two-phase flows [1]. This model requires the user to specify the single-phase turbulent mixing coefficient, β, as input. Previous single-phase turbulent mixing model assessments [11] using the Kumamoto University 2×3 facility data [16] have yielded an optimal single-phase mixing coefficient of 0.007, so this value was used in this study. However, sensitivity to the model choice was also assessed. CTF uses the Lahey-Moody model for estimating void drift. This also requires a modeling coefficient, K_a, to be input by the user. This was set to the suggested default value of 1.4 [17].

Modeled tests included four single-phase cases and 13 two-phase cases. In the facility, an isokinetic flow splitter measurement technique was used to split the flow of the corner, side, and inner channels from one another so that mass flux and temperature measurements could be taken at the outlet of the individual channel types. The single-phase case results are shown in Fig. 8. The experimental measurement uncertainty was estimated to be 2 % for mass flux measurements [12]; however, error bars of ±5 % are shown to better illustrate the spread in the data. Statistics shown in the plot include the mean relative error (i.e., the average of the relative error for every measurement point) for each channel type and all measurements. The standard deviation of the relative error is also shown. As indicated in the figure, the side and inner channel type predictions are very good. The corner predictions are less accurate, but the margin of error is still less than 5 %.
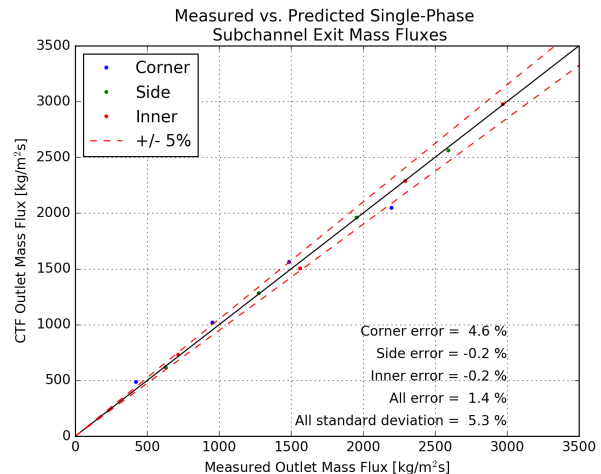
The two-phase case results are shown in Fig. 9. The

Fig. 8. CTF prediction of GE 3×3 facility single-phase exit mass flux distribution.
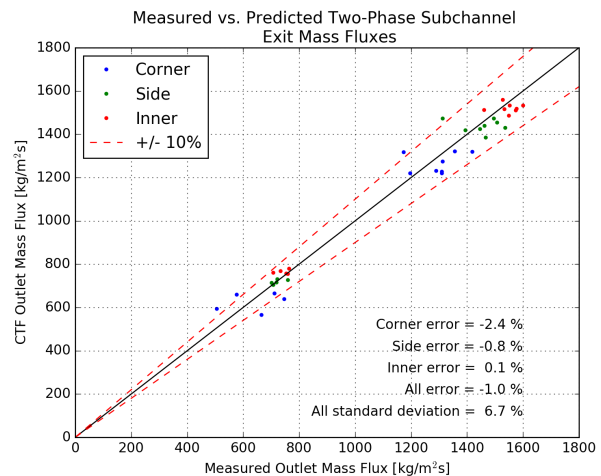

Fig. 9. CTF prediction of GE 3×3 facility two-phase exit mass flux distribution.

scatter of the data increases, as observed visually and by the increase in the standard deviation. The corner channel type continues to be the least accurately predicted. Overall, the data still clusters closely around the mean. The exit quality comparison for the two-phase cases is shown in Fig. 10. Experimental measurement uncertainty for quality was estimated to be 0.02. Error bands are placed at 0.05 in the figure. It is observed that inner and side channel type predictions are within 5 % quality of experimental results for the most part. Again, the corner channel types are least accurate, and it is observed that quality is typically overpredicted. These findings are consistent with other COBRA-TF version models of the GE 3×3 facility found in the literature [18].

Table II shows the sensitivity of the mean relative error and standard deviation to the void drift model and the turbulent mixing model. The first column provides the results shown in Fig. 8–10. The second column presents statistics when the void drift model is disabled. The third column shows results
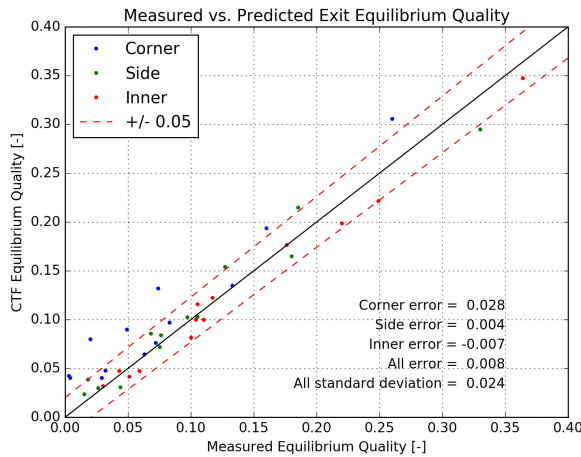
Fig. 10. CTF prediction of GE 3 × 3 facility exit equilibrium quality distribution.

TABLE III. Sensitivity of quality distribution to turbulent mixing coefficient and void drift model

Channel	Void drift on	Void drift off	R&R
	Mean Error		
Corner	0.028	0.082	0.026
Side	0.004	0.007	0.005
Inner	−0.007	−0.020	−0.008
All	0.008	0.023	0.008
	Mean Standard Deviation		
All	0.024	0.065	0.023

TABLE II. Sensitivity of two-phase mass flux results to turbulent mixing coefficient and void drift model

Channel	Void drift on	Void drift off	R&R
	Mean Error		
Corner	−2.4	−21.8	−0.1
Side	−0.8	−1.3	−0.9
Inner	0.1	3.7	−0.3
All	−1.0	−6.5	−0.4
	Mean Standard Deviation		
All	6.7	18.4	6.6

when the void drift model is re-enabled and the mixing model is switched to the Rogers and Rosehart option in CTF, which dynamically calculates the single-phase turbulent mixing coefficient as a function of flow conditions and geometry. The results indicate that this model causes results to cluster better around the experimental results; however, it has been observed that the model tends to overpredict the single-phase mixing coefficient in single phase flows. For example, Fig. 11 shows that the mean error and standard deviation both increase for the single phase cases when the Rogers and Rosehart model is employed.

2. BFBT Facility

The BFBT facility was an electrically heated 8 × 8 rod bundle facility representative of BWR geometry and operating conditions. The tests included several experimental configurations. The lateral geometry is summarized in Fig. 12 along with the CTF channel layout scheme. The black rods are water rods, and the gray rods are heater rods that were shut off for particular assembly configurations. Assembly types 0-1, 0-2, 0-3, and 1 used lantern type spacer grids, while assembly type 4 used a ferrule type grid. The axial and radial power shapes are uniform for assembly types 0-1, 0-2, and 0-3. The axial
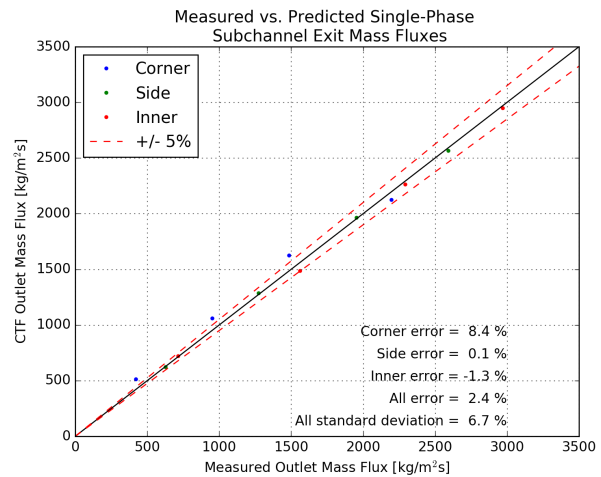

Fig. 11. CTF prediction of GE 3 × 3 facility single-phase exit mass flux distribution using the Rogers and Rosehart model in place of a constant β value of 0.007.
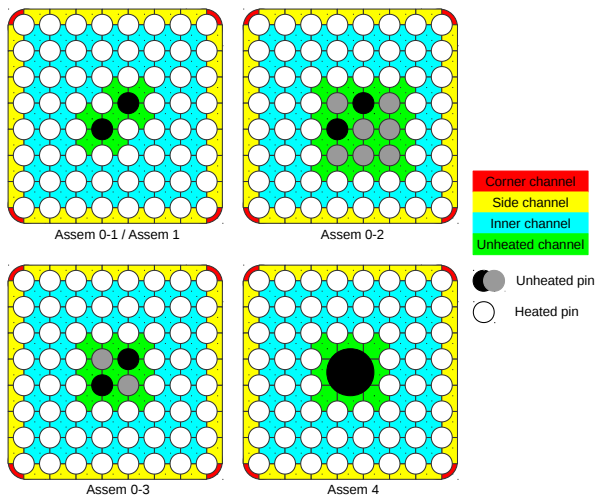
Fig. 12. BFBT assembly types included in CTF assessment and channel grouping scheme.

TABLE IV. BFBT void distribution test conditions

Test	Pressure	Inlet Subcooling	Flow Rate	Power
	[MPa]	[kJ/kg]	[ton/h]	MW
0011-55	7.180	52.60	54.03	1.90
0011-58	7.172	51.00	54.90	3.51
0011-61	7.210	50.90	54.79	6.44
0021-16	7.190	54.00	54.85	1.91
0021-18	7.171	49.80	54.90	3.51
0021-21	7.179	51.40	54.90	6.45
0031-16	7.180	52.40	54.96	1.92
0031-18	7.179	50.00	54.79	3.52
0031-21	7.171	49.40	54.90	6.45
1071-55	7.191	52.80	54.61	1.92
1071-58	7.158	50.30	55.07	3.52
1071-61	7.200	51.80	54.65	6.48
4101-53	7.181	52.80	54.65	1.24
4101-55	7.195	52.90	54.59	1.92
4101-58	7.152	50.60	54.58	3.52
4101-61	7.180	52.50	54.65	6.48

shape is uniform for assembly type 4, but its radial power shape is non-uniform. Assembly 1 has a cosine-shaped axial power profile and a nonuniform radial power profile.

CTF form losses were set using calculations from the BFBT workshop [19]. The turbulent mixing and void drift model were set to the same parameters as for the GE 3 × 3 study. The CTF axial mesh size was 3.6 mm on average.

The BFBT experiments included several different types of tests, including single- and two-phase pressure drop measurement cases, void distribution measurement cases, critical power measurement cases, and transient cases. The void distribution cases are modeled in this study. Operating conditions for the 16 tests that were modeled are shown in Table IV.
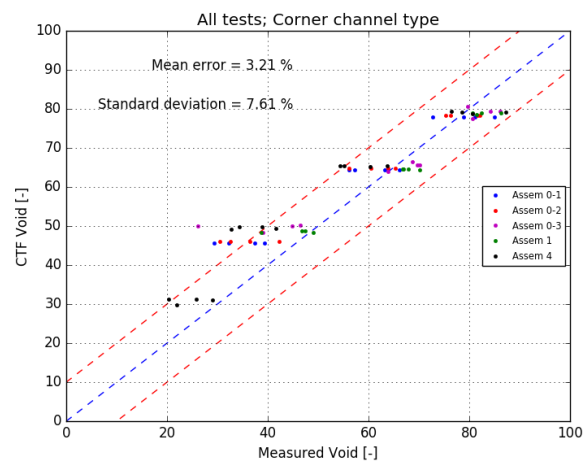

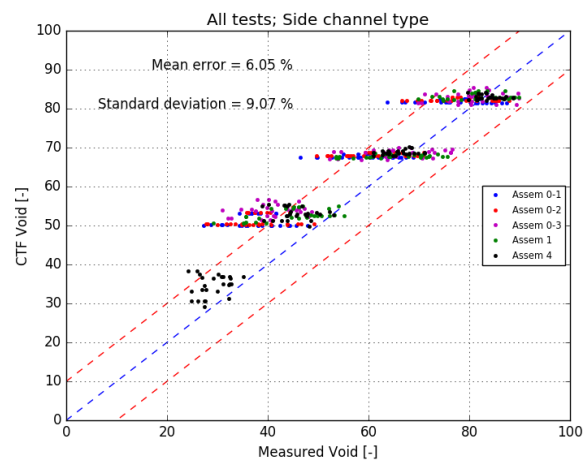Fig. 13. Comparison of CTF predictions and BFBT void measurements for corner channel type.

Fig. 14. Comparison of CTF predictions and BFBT void measurements for side channel type.

For the void distribution cases, x-ray computed tomography measurements were made above the end of the heated length of the facility to determine the high-resolution outlet void distribution. These measurements were averaged on a per-coolant-channel basis so they could be used for subchannel code validation exercises.

The predicted exit void fraction distribution was compared to the experimental results. Results were grouped by subchannel type, and four categories were created for this study (Fig. 12). A comparison of the measured and predicted results is shown for the corner, side, inner, and near-unheated channel types in Figs. 13–16.

Figures 13–16 show 10 % error bars. The mean error (CTF minus experimental void) and standard deviation of the error is shown in the figures. A few conclusions can be drawn from the data. First, the scatter in the experimental data is much larger than in CTF as evidenced by the horizontal "striping" in the data. As assembly types 0-1 and 4 are almost
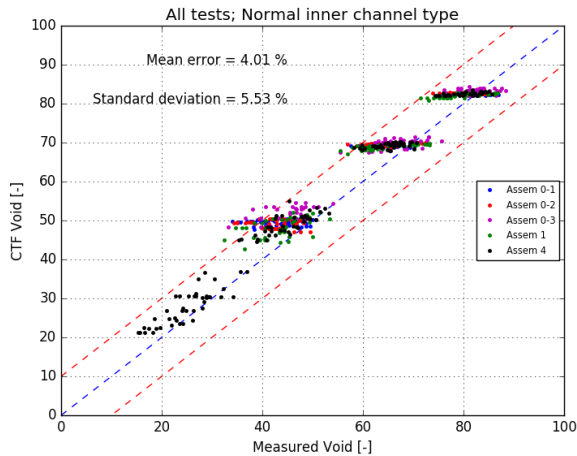
Fig. 15. Comparison of CTF predictions and BFBT void measurements for inner channel type.
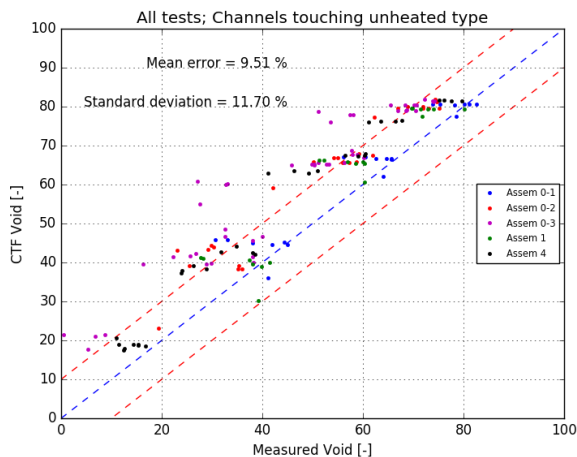

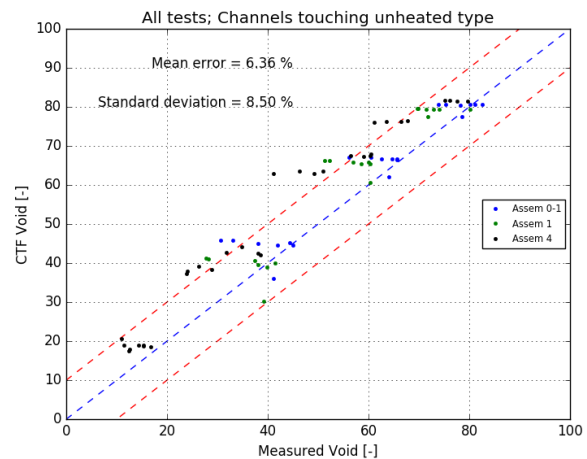Fig. 16. Comparison of CTF predictions and BFBT void measurements for the near-unheated channel type.

Fig. 17. Comparison of CTF and BFBT measurements for channels that touch unheated rods (neglect data from assembly 0-2 and 0-3).

symmetrical, this indicates the experimental measurement uncertainty may be larger than the 3 % quoted in the benchmark specification.

Second, CTF tends to overpredict the void for every channel category. The mean error is always positive, showing that the bundle-average void is overpredicted in all cases. It is likely that the interfacial drag calculation is inaccurate, which leads to an inaccurate void prediction. This seems to be especially true for the slug flow regime (i.e., the void between 0.2–0.5 in the CTF flow regime map). After that, the churn-turbulent regime is the next least accurate (void greater than 0.5 and less than either 0.8 or the film stability limit). The churn-turbulent regime does not actually have its own set of closure models; rather, it is a linear interpolation between the interfacial area, drag, and heat transfer of the slug and annular mist flow regimes, which may explain the carryover of the inaccuracies from the slug regime.

The slug flow regime interfacial area and drag model is a mechanistic model with several critical assumptions: 1) small bubble void is 0.2, 2) large bubbles are spherical in shape, 3) large bubble drag can calculated assuming they exist in the Newton regime, and 4) the interfacial area and drag can be linearly interpolated based on local calculated void fraction. If any of these assumptions are incorrect, the model may produce erroneous results. In the future, the PWR Subchannel and Bundle Tests (PSBT) single-channel tests [20] will be used to perform more of a separate effects validation of the CTF interfacial drag models and to help determine how the closure models might be further improved.

Third, the near-unheated conductor region is clearly the most poorly predicted channel category. Void is most severely overpredicted for the channels between the four unheated rods. Figure 17 eliminates assembly types 0-2 and 0-3 and demonstrates that mean error and standard deviation drops considerably when these channel types are excluded.

The CTF void predictions are mostly within 10 %–15 % void of experimental measurements. The trends observed in this study are consistent with the results observed in an earlier

TABLE V. Summary of statistics for CTF and BFBT comparisons

Category	Mean error (%)	Standard deviation (%)
Corner	3.2	7.6
Side	6.1	9.1
Inner	4.0	5.5
Unheated	9.5	11.7
All	6.2	8.8

study that used an older version of CTF that predated CASL [21]. Overall statistical results for the BFBT void distribution assessment are summarized in Table V.

VI. CONCLUSIONS

This paper presents work completed to prepare CTF for modeling BWR problems in CASL. Three primary tasks have been undertaken, which include creating a new preprocessor utility for converting the VERAIn common input file BWR models into native CTF input decks, implementing an outer iteration loop in CTF for balancing the pressure drop in the fuel assemblies so that large-scale pin-resolved models can be run in reasonable computational times, and expanding the CTF V&V document to include two-phase experiments.

The outer iteration loop that was added uses a linear curve fit of bundle pressure drop to inlet flow rate data from successive iterations to predict the required mass flow rate in each assembly to obtain a single consistent core pressure drop. This feature has been tested for a full-core mock BWR/4 model with nonuniform power distribution. The individual assembly pressure drops converged to within 0.05 psi of the core average in five outer iterations in about 45 min on the OLCF Titan cluster.

The two-phase assessments were performed using the GE 3×3 and BFBT 8×8 facilities. Results from the GE 3×3 facility showed that corner-type channels are the least accurately predicted, but in general, CTF predictions agreed with experimental quality and mass flux distributions within a reasonable degree. The BFBT assessment shows that CTF tends to overpredict the void, which is likely because of inaccuracies in the interfacial drag models employed by the code. When all data points are considered, CTF tends to overpredict the experimental data by 6.2 % void. The greatest error was found for channels surrounded by four unheated pins. The findings of this study are consistent with assessments of older versions of CTF that predated the CASL program and all associated code changes.

Future work will focus on expanding the preprocessor to include support for partial-length rods and studies will be performed to investigate the modeling needs for the bypass flow in the core. Strategies for accelerating the pressure outer iteration loop will also be investigated. Using a simple drift-flux solver to formulate a better initial pressure distribution may help eliminate some outer iterations and reduce the total BWR core solve time. Finally, work is underway to further expand the CTF two-phase assessment, and investigations are also underway to determine how to improve the two-phase closure models in the code.

VII. ACKNOWLEDGMENTS

REFERENCES

1. R. SALKO and M. AVRAMOVA, *CTF Theory Manual*, The Pennsylvania State University.
2. M. THURGOOD, J. KELLY, T. GUIDOTTI, R. KOHRT, and K. CROWELL, "COBRA/TRAC - A Thermal-Hydraulics Code for Transient Analysis of Nuclear Reactor Vessels and Primary Coolant Systems Equations and Constitutive Models," Tech. Rep. NUREG/CR-3046, PNL-4385, Pacific Northwest National Laboratory (1983).
3. R. SALKO, M. AVRAMOVA, R. HOOPER, S. PALM-TAG, E. POPOV, and J. TURNER, "Improvements, Enhancements, and Optimizations of COBRA-TF," in "International Conference on Mathematics and Computational Methods (M&C)," (2013).
4. R. SALKO, R. SCHMIDT, and M. AVRAMOVA, "Optimization and Parallelization of the Thermal-Hydraulics Sub-channel Code CTF for High-Fidelity Multi-physics Applications," *Annals of Nuclear Energy* (2014), accepted for publication.
5. R. SALKO, T. LANGE, V. KUCUKBOYACI, Y. SUNG, S. PALMTAG, J. GEHIN, and M. AVRAMOVA, "Development of COBRA-TF for Modeling Full-Core Reactor Operating Cycles," in "Advances in Nuclear Fuel Management V (ANFM 2015), Hilton Head Island, South Carolina, USA," (2015).
6. U. OF MICHIGAN, *MPACT Theory Manual* (2013).
7. B. KOCHUNAS, D. JABAAY, S. STIMPSON, A. GRAHAM, T. DOWNAR, B. COLLINS, K. KIM, W. WIESELQUIST, K. CLARNO, J. GEHIN, and S. PALMTAG, "VERA Core Simulator Methodology for PWR Cycle Depletion," Tech. Rep. CASL-U-2015-0155-000, Consortium for Advanced Simulation of Light Water Reactors (2015).
8. B. COLLINS, R. SALKO, S. STIMPSON, K. CLARNO, and A. GODFREY, "Simulation of Crud Induced Power Shift using the VERA Core Simulator and MAMBA," in "PHYSOR 2016," (2016).
9. R. PAWLOWSKI, K. CLARNO, R. MONTGOMERY, R. SALKO, T. EVANS, J. TURNER, and D. GASTON, "Design of a High Fidelity Core Simulator for Analysis

of Pellet Clad Interaction," in "ANS MC2015âĂŤJoint International Conference on Mathematics and Computation (M&C), Supercomputing in Nuclear Applications (SNA) and the Monte Carlo (MC) Method, Nashville, TN, American Nuclear Society, LaGrange Park," (2015).

10. S. PALMTAG and A. GODFREY, "VERA Common Input User Manual," Tech. Rep. CASL-U-2014-0014-002, Consortium for Advanced Simulation of Light Water Reactors (2014).

11. R. SALKO, T. BLYTH, C. DANCES, J. MAGEDANZ, M. GERGAR, C. GOSDIN, M. AVRAMOVA, S. PALMTAG, and J. GEHIN, *CTF Validation and Verification*, The Pennsylvania State University (2015).

12. D. W. R. R. T. LAHEY JR., B. S. SHIRLAKAR, "Two-Phase Flow and Heat Transfer In Multirod Geometries: Subchannel and Pressure Drop Measurements in a Nine-Rod Bundle for Diabatic and Adiabatic Conditions," Tech. rep., General Electric (1970).

13. B. NEYKOV, F. AYDOGAN, L. HOCHREITER, K. IVANOV, H. UTSUNO, and F. KASAHARA, "NUPEC BWR Full-size Fine-mesh Bundle Test (BFBT) Benchmark," Tech. rep., NUCLEAR ENERGY AGENCY (2006).

14. M. AVRAMOVA, *Development of an Innovative Spacer Grid Model Utilizing Computational Fluid Dynamics within a Subchannel Analysis Tool*, Ph.D. thesis, The Pennsylvania State University (2007).

15. M. AVRAMOVA, A. VELAZQUEZ-LOZADA, and A. RUBIN, "Comparitive Analysis of CTF and TRACD Thermal-hYdraulic Codes Uinsg OECD/NRC PSBT Benchmark Void Distribution Database," *International Journal of Science and Technology of Nuclear Installations* (2013), article ID: 725687.

16. M. SADATOMI, A. KAWAHARA, K. KANO, and Y. SUMI, "Single- and Two-Phase Turbulent Mixing Rate between Adjacent Subchanels in a Vertical 2x3 Rod Array Channel," *International Journal of Multiphase Flow*, **30**, 481–498 (2004).

17. N. TODREAS and M. KAZIMI, *Nuclear Systems II Elements of Thermal Hydraulic Design*, Hemisphere Publishing Corporation (1990).

18. *COBRAG Subchannel Analysis of BWR Fuel Thermal Hydraulic Performance* (September 2010).

19. M. GLÜCK, "Contributions with the sub-channel code F-COBRA-TF to the NUPEC BWR Full-Size Fine-Mesh Bundle Test (BFBT) Benchmark (Exercises I-1 and II-0)," in "Second Workshop on OECD/NRC Benchmark based on NUPEC BWR Full-size Fine-mesh Bundle Tests (BFBT), Pisa (Italy), 26–27 April 2006," (2006).

20. A. RUBIN, A. SCHOEDEL, M. AVRAMOVA, H. UTSUNO, S. BAJOREK, and A. VELAZQUEZ-LOZADA, "OECD/NRC BENCHMARK BASED ON NUPEC PWR SUBCHANNEL AND BUNDLE TESTS (PSBT)," Tech. rep., US NRC and OECD Nuclear Energy Agency (2010).

21. M. AVRAMOVA, K. IVANOV, and L. HOCHREITER, "Analysis of Steady State and Transient Void Distribution Predictions for Phase I of the OECD/NRC BFBT Benchmark using CTF/NEM," in "The 12th International Topical Meeting on Nuclear Reactor Thermal Hydraulics (NURETH-12)," (2007).